Isotopic exchange processes in cold plasmas of H_2/D_2 mixtures

Miguel Jiménez-Redondo, Esther Carrasco, Víctor J. Herrero,* Isabel Tanarro*

Inst. Estructura de la Materia, CSIC

Serrano 123, 28006 Madrid, Spain

Corresponding authors: vherrero@iem.cfmac.csic.es, itanarro@iem.cfmac.csic.es

Abstract

Isotope exchange in low pressure cold plasmas of H_2/D_2 mixtures has been investigated by means of mass spectrometric measurements of neutrals and ions, and kicm^{-3} s^{-1} cm^{-3} s^{-1} tic model calculations. The measurements, which include also electron temperatures and densities, were performed in a stainless steel hollow cathode reactor for three discharge pressures: 1, 2, and 8 Pa, and for mixture compositions ranging from 100% H_2 to 100% D_2. The data are analyzed in the light of the model calculations, which are in good global agreement with the experiments. Isotope selective effects are found both in the surface recombination and in the gas-phase ionic chemistry.

The dissociation of the fuel gas molecules is followed by wall recycling, which regenerates H_2 and D_2 and produces HD. Atomic recombination at the wall is found to proceed through an Eley-Rideal mechanism, with a preference for reaction of the adsorbed atoms with gas phase D atoms. The best fit probabilities for Eley Rideal abstraction with H and D are: $\gamma_{ER\ H}=1.5\times10^{-3}$, $\gamma_{ER\ D}=2.0\times10^{-3}$. Concerning ions, at 1 Pa the diatomic species H_2^+, D_2^+ and HD^+, formed directly by electron impact, prevail in the distributions, and at 8 Pa, the triatomic ions H_3^+, H_2D^+, HD_2^+ and D_3^+, produced primarily in reactions of diatomic ions with molecules, dominate the plasma composition. In this higher pressure regime, the formation of the mixed ions H_2D^+ and HD_2^+ is favoured in comparison with that of H_3^+ and D_3^+, as expected on statistical grounds. The model results predict a very small preference, undetectable within the precision of the measurements, for the generation of triatomic ions with a higher degree of deuteration, which is probably a residual influence at room temperature of the marked zero point energy effects (ZPE), relevant for deuterium fractionation in interstellar space. In contrast, ZPE effects are found to be decisive for the observed distribution of monoatomic ions H^+ and D^+, even at room temperature. The final H^+/D^+ ratio is determined to a great extent by proton (and deuteron) exchange, which favours the enhancement of H^+ and the concomitant decrease of D^+.

1. Introduction

Plasmas containing hydrogen and its isotopes are of paramount importance in controlled fusion devices [1,2], planetary atmospheres [3,4] and interstellar space [5,6]. Valuable insights into the chemistry of these low collisionality environments, which is mostly driven by heterogeneous processes at surfaces, and by barrierless ion-molecule reactions in the gas phase, can be gained from the investigation of isotopic exchange in low pressure laboratory plasmas.

The formation of H_2 in a surface reaction between hydrogen atoms is of relevance in many technological processes like thin film processing [7] and notably in nuclear fusion reactors, where it is determinant for fuel recycling [1]. It is also crucial on interstellar cloud grains [8,9], the assumed birthplace of most of the existing molecular hydrogen. Consequently, the dynamics of hydrogen at surfaces has been intensively studied (see for instance [10-15] and references therein). Two main mechanisms named respectively Langmuir-Hinshelwood (LH) and Eley-Rideal (ER) are conventionally recognized in surface reactions [16,17]. In the LH mechanism, reaction takes place between thermalized adsorbed chemical species diffusing over the surface. Laboratory experiments and models [12,18] have shown that, at the very low temperatures of interstellar grains, this mechanism is probably responsible for most of the recombination of physisorbed H atoms to form H_2. Langmuir-Hinshelwood reactions involving chemisorbed H atoms can also take place on higher temperature objects in space [13]. The ER mechanism assumes the direct abstraction of an adsorbed (usually chemisorbed) species by an incoming gas phase reactant. The actual occurrence of this mechanism in the surface recombination of H_2 was convincingly demonstrated in a series of high resolution molecular beam experiments [19-21]. Sometimes the ER recombination is not immediate, and the impinging H atom can get trapped temporarily in a hot precursor state at the surface before reacting through a so called hot atom (HA) or Harris-Kasemo [22,23] mechanism. The concurrence of different mechanisms is a general feature of surface reactions and the predominance of a given one is mostly a matter of the particular circumstances [24]. The ER mechanism has often been found to be of great relevance in H_2 plasma reactors [15], which are characterized by a large flux of H atoms to the walls and a high surface coverage. A characteristic isotope effect, which renders the abstraction of adsorbed hydrogen atoms, H(s), by gas phase D atoms more efficient than the reverse process, is generally found in the ER recombination of hydrogen (see [14,25] and references therein). A simple impulsive model [26] showing that the interaction time, and thus the reaction probability, is larger in the heavy-light D+H(s) combination than in light-heavy H+D(s) collisions is often invoked to rationalize qualitatively the observations. However, the actual magnitude of the effect is system dependent and is determined by a complex

dynamics including, both, the energy transfer from the incoming gas phase atom to the adsorbed atom, and the coupling of the adsorbed atom to the surface [14].

Gas phase ion molecule reactions are thought to be largely responsible for the strong enrichment in deuterium containing molecules observed in cold interstellar regions [6,27-31]. In general, this type of reactions have no dynamical barrier, but they may have an "energetic" barrier associated with the different zero point energies (ZPE), i.e., the different ground state energies of the molecular species (reactants and products) [6]. In the case of H/D exchange, ZPE constraints favour species with higher deuteration. A key process in interstellar clouds is the reaction between the most abundant ion, H_3^+, and the most abundant D containing molecule, HD. This reaction produces H_2D^+, which is the initiator of an extensive deuteration chain. Under conditions of high depletion, when most of the molecules acting as sinks of H_2D^+ are condensed on the surface of dust grains, the deuteration chain can continue to HD_2^+ and D_3^+. Astronomical observations of H_2D^+ [32] and more recently of HD_2^+ [33] support this picture of deuterium fractionation. Laboratory experiments and theoretical calculations, aimed at the determination of the rate coefficients for the reactions of the mentioned triatomic ions with H_2 molecules and its isotopic variants, were reported by several groups [28,29,34-40], with special attention to the low temperature range characteristic of interstellar space. The results, not always free from controversy, stimulated a rich debate on the validity of thermodynamic models for the estimation of rate coefficients and on the importance of nuclear spin restrictions and state resolved rate constants in very cold environments. A state of the art discussion of progress in this field can be found in reference [41]. Room temperature rate constants, either measured or derived from thermodynamic arguments [34,42,43] are not so controversial, but they have not been subjected to such a detailed scrutiny as their low temperature counterparts and it is worth investigating whether they can in fact account for the kinetics of relatively complex mixtures involving the different H_x^+ ions (with x=1-3) and its isotopic variants. Although fractionation effects are expected to be especially relevant at very low temperatures, they cannot be totally excluded *a priori* in room temperature plasmas, given the comparatively large ZPE differences between some of the isotopic variants of hydrogen molecules and ions.

With the aim of investigating isotope exchange processes in room temperature hydrogen plasmas, we have carried out a detailed diagnostics and modelling of hollow cathode (HC) discharges of H_2, D_2, and H_2/D_2 mixtures. The present study extends significantly our previous works on glow discharges of pure H_2 [44,45]. Over the pressure range studied (1-8 Pa) large changes in the composition of the plasma are observed and the key physicochemical processes responsible for these composition changes are identified with the help of a simple model that provides a good overall picture of the discharge kinetics. Distinct isotopic effects, both at the walls and in the gas phase, are especially addressed in the discussion.

2 Experimental

The experimental set-up has been described in detail in previous publications [44,46] and only the details relevant to the present work will be given here. The experiments have been carried out in a stainless steel grounded hollow cathode DC reactor (10 cm diameter, 34 cm length) with a central anode. A quadrupole mass spectrometer (Balzers, Prisma QMS 200) installed in a differentially pumped vacuum chamber was used to sample neutral species from the plasma through a ~ 100 μm diaphragm, and a plasma process monitor (Balzers PPM421) with a quadrupole mass filter and an ion energy analyzer, placed in another differentially pumped vacuum chamber, was employed for mass and energy resolved detection of ions, which are extracted directly from the plasma through a 100 μm diameter orifice at the top of the cathode. During operation, the pressures in the two detection chambers were kept in the 10^{-5} Pa range by means of their respective turbomolecular and dry pump systems. Electron temperatures and charge densities were measured with a double Langmuir probe.

Steady-state plasma currents ~ 150 mA and voltages ~ 300 – 450 V (depending on gas composition and pressure) were maintained during the experiments. An electron gun was employed for plasma ignition.

Pure H_2 and D_2 as well as H_2/D_2 mixtures were used for plasma generation. Experiments were performed for total reactor pressures of 1, 2 and 8 Pa, as measured with a capacitance manometer. Five mixture proportions, with approximate $H_2/(H_2+D_2)$ ratios of 0.0, 0.25, 0.50, 0.75, and 1.00 were studied for each pressure. The desired pressure and gas mixture composition were selected by balancing the input and output flows for each gas, by means of two needle valves in the respective H_2 and D_2 gas inlets and a butterfly valve placed at the gas exit between the reactor and its vacuum system, a turbomolecular pump backed by a dry pump. Residence times for H_2 and D_2, calibrated according to [44,47], were 0.18 s for 1-2 Pa and 0.40 s for 8 Pa, with typical uncertainties of 25%. The H_2/D_2 ratios before turning on the discharges were checked by measuring the peak intensities at 2 and 4 a.m.u. with the Prisma mass spectrometer, previously calibrated for the pure gases, subtracting background signals. The relative sensitivity of the detection system for neutrals (including sampling diaphragm, differential pumping and QMS) was determined by comparing the reactor chamber pressures, measured with the capacitance manometer for samples of pure H_2 and D_2, with the corresponding QMS readings for masses 2 and 4. The value for HD (mass 3) was interpolated.

Total ion fluxes were obtained, as described in previous works [46,48,49], by integrating the ion energy distributions recorded with the plasma monitor. Relative ion concentrations in the plasma

were derived by multiplying the ion fluxes by the corresponding square roots of their masses. The relative sensitivity of the plasma monitor (including electrical filters and electron multiplier) to H_2^+ and D_2^+ was checked by filling the chamber of the PPM421 with small pressures of H_2 and D_2 (~ 10^{-4} Pa) and comparing in each case the PPM signals for masses 2 and 4, weighted by the respective ionization cross section at the chosen electron energy (70 eV), with the chamber pressure, as determined from the reading of a Bayard-Alpert gauge with the appropriate correction factor [46]. No significant variations in the sensitivity of the plasma monitor were observed for these two masses and it was assumed that the sensitivity was roughly constant, within the experimental uncertainty, over the comparatively narrow range of masses (1-6) investigated.

Charge densities, n_e, and electron temperatures, T_e, were measured for pure H_2 and D_2 plasmas with the Langmuir probe, assuming Maxwellian distributions and weighting for the relative ion composition in each case. The results can be seen in table 1.

3 Kinetic model

We have used a zero order kinetic model to simulate the ion and neutral chemistry of our H_2 + D_2 plasmas. The model consists of a set of time resolved coupled differential equations which account for the different reactions taking place in the plasma glow and at the reactor walls. These equations are then numerically integrated to obtain the time evolution and the steady state concentrations for the various species considered.

This model requires certain input parameters: the pressure in the plasma reactor, the pressure dependent electron density and temperature (assuming a Maxwellian distribution for the electron energy), the H_2/D_2 ratio and the residence times for the precursors; all of which have been determined experimentally. The best simulation of the experimental results was obtained with residence times somewhat lower (0.12 s for 1 and 2 Pa, and 0.30 s for 8 Pa) than the measured ones. The electron temperature in the individual simulations was also fit to the data. The optimized values did not differ by more than 15% from the measured T_e and were thus well within the experimental uncertainty (see table 1). It should be stressed here that the assumption of a Maxwellian electron energy distribution, $f(E_e)$, is just an approximation. More rigorous treatments of the plasma include a coupling between the electron kinetics and that of the heavier species (see for instance refs [50-52]) and lead in general to deviations from the Maxwellian behaviour in the high energy tail; however, in the case of pure H_2 plasmas, the calculated $f(E_e)$ may not differ much from a Maxwellian curve [51] and, in fact, in previous works [44, 53], the chemistry of the heavier species in hydrogen plasmas has been satisfactorily described with this assumption.

The different processes considered, together with their corresponding room temperature rate coefficients, are listed in tables 2 and 3. They include electron impact dissociation and ionization, charge transfer, wall neutralization and chemical reactions, both in the gas phase (ion molecule reactions) and at the walls. The sources for the rate coefficients used are indicated in the table caption. Most of them have been taken from [53] and our previous work [44], from the compilation of Anicich [43], and from the article of Giles et al. [34] for the reactions of triatomic ions with diatomic molecules.

The dynamics of vibrational excitation and de-excitation of the H_2 molecules is not included explicitly in the model, but estimates based on emission spectroscopy data in conjunction with a collisional radiative model suggest that the vibrational populations in our plasmas are concentrated in the lower levels and can be roughly described by a vibrational temperature, T_v, of ~ 3000 K [44,53]; a correction for this molecular T_v is already incorporated in the pertinent rate constants values taken from refs [44,53]. The use of a (Boltzmann) vibrational temperature is again an approximation. Models including the kinetics of the individual vibrational states [50-52] produce deviations from the Boltzmann distribution, which can be manifest as plateaus (i.e. similar probabilities) for the relative population of a given set of levels. But these effects are often restricted to some excited, sparsely populated states and, for many purposes, the use of a vibrational temperature is still adequate as shorthand for the description of the vibrational excitation.

Negative H^- or D^- ions can be formed in hydrogen plasmas and, in fact, there is great interest in the development of sources of negative H and D ions based on different types of hydrogen discharges (see for instance ref. [54] and references therein). However, the production of negative atomic ions, usually through dissociative electron attachment to H_2 molecules, requires in general slow electrons and molecules in highly excited vibrational levels (especially v> 4), which are scarce in our plasmas. Recent estimates based on model calculations and photodetachment measurements [55] indicate that the concentration of H^- in a hollow cathode discharge of H_2 is orders of magnitude lower than that of electrons. Consequently, we have not considered negative ions and have assumed that electrons are the only negative charge carriers of our plasmas.

Collisions between ions and electrons, which where included in a previous version of the model [44], have now been removed. They have large rate coefficients, k_{neu} (in the 10^{-8} cm^{-3} s^{-1} range), and are assumed to play a decisive role in the destruction of positive ions in interstellar space [56], where other neutralization mechanisms like surface reactions are much less important but they have been verified to be irrelevant for the dimensions of our reactor, due to the very low concentrations of ions and electrons (~ 10^{10} cm^{-3}). In fact, these reactions in our reactor would occur only with very long characteristic times $(k_{neu} \times n_e)^{-1}$ ~ 0.01 s. Under our experimental conditions, the ions produced in the plasma are either transformed in reactions with the much more abundant

neutral species (with typical densities, N, in the 10^{13}-10^{14} cm^{-3} range and rate coefficients, k_{M_i}, in the range of 10^{-9} cm^{-3} s^{-1}) (see table 2), or neutralized, with virtually unit probability, at the reactor wall (i. e., at the cathode). The typical characteristic times of these two kinds of processes are in fact $(k_{M_i} \times N)^{-1} \sim 10^{-4}$ -10^{-5} s, and $\tau_i \sim 10^{-6}$ s (see equation 1 below), respectively.

The loss of ions from the plasma glow is modelled by taking into account that ion generation and disappearance must be balanced in the plasma volume in order to meet the electroneutrality condition. With this consideration, the (first order) rate constant for the loss of a given ionic species i from the plasma (see references [44,57] for details) can be expressed as:

$$k_i = \tau_i^{-1} = \frac{\sum_j [X_j] n_e k_j}{\sqrt{m_i} \sum_{l=1} \frac{[Y_l]}{\sqrt{m_l}}} \qquad (1)$$

The sum in j in the numerator represents the total rate of ionization. In this expression, $[X_j]$ is the density of the neutral species being ionized and k_j the corresponding ionization rate constant (or sum of rate constants, if more than one process can contribute to the ionization of a given neutral species). The sum in l in the denominator accounts for the different ionic species, and m_l and $[Y_l]$ are the mass and density of ion l respectively. The inverse dependence of ion mobility on the square root of the ion mass is also reflected in equation (1).

We have considered that wall recombination of neutral atoms takes place in two steps: first, atomic adsorption at the wall, and then, chemical reaction between atomic species, which could proceed in principle either by an Eley-Rideal or by a Langmuir-Hinshelwood mechanism. Once formed, molecular species are assumed to be desorbed instantly.

The rate of change of the gas phase density of atomic species X due to adsorption is given by [58]:

$$\frac{d[X]}{dt} = -k_{ads\,X} \cdot [X] \left(1 - \frac{X_S + Y_S}{C_{sat}}\right) \qquad (2)$$

Where X_s and Y_s are the sites occupied by one of the two types of atoms (in our case H or D indistinctly) and C_{sat}, the surface saturation concentration, is the total number of possible free sites per surface unit, for which we have assumed a value: $C_{sat} = 10^{15}$ cm^{-2} [10]. The rate constant for adsorption $k_{ads\,X}$ is given by [44]:

$$k_{ads\,X} = 1/t_{T\,X}\ , \text{ with } \quad t_{T\,X} = t_{dif\,X} + t_{ads\,X} \qquad (3)$$

where $t_{dif\ X}$ and $t_{ads\ X}$ are the characteristic times for diffusion to the wall and adsorption on the surface, respectively. The diffusion time can be expressed as [59]:

$$t_{dif} = \frac{\Lambda^2}{D_X} \tag{4}$$

where Λ is the characteristic diffusion length in the reactor and D_x is the diffusion coefficient for X atoms. The corresponding expression for $t_{ads\ X}$ is given by [59,60]:

$$t_{ads\ X} = \frac{4 \cdot V_R \cdot \left(1 - \frac{\gamma_{ads\ X}}{2}\right)}{A \cdot \gamma_{ads\ X} \cdot \langle v_{tX} \rangle} \tag{5}$$

where V_R and A are the volume and area of the reactor, respectively, and $\langle v_{tX} \rangle$, the mean thermal speed of the atom. We have further assumed that for our system $\gamma_{ads\ X} = 1$, in all cases.

The contribution of gas-phase X atoms to the rate of formation of XY molecules by an Eley-Rideal mechanism is given by:

$$\frac{d[XY]}{dt} = k_{ER\ XY}[X]\frac{Y_S}{C_{sat}} \tag{6}$$

where the ratio Y_s/C_{sat} gives the fraction of wall sites covered with adsorbed Y atoms. The corresponding ER rate coefficient is given by:

$$k_{ER\ XY} = 1/t_T \quad \text{with} \quad t_T = t_{dif\ X} + t_{ER\ XY} \tag{7}$$

where $t_{ER\ XY}$ is the characteristic time for the Eley–Rideal reaction that, in a similar way to (5), can be expressed as:

$$t_{ER\ XY} = \frac{4 \cdot V_R \cdot \left(1 - \frac{\gamma_{ER\ XY}}{2}\right)}{A \cdot \gamma_{ER\ XY} \cdot \langle v_{tX} \rangle} \tag{8}$$

For the molecules considered in this work, the values giving a best fit to the data were: $\gamma_{ER\ H_2} = \gamma_{ER\ HD} = 0.0015$ and $\gamma_{ER\ D_2} = \gamma_{ER\ DH} = 0.002$.

For the Langmuir-Hinshelwood mechanism, reaction takes place only between adsorbed atoms, and its contribution to XY formation can be written as.

$$\frac{d[XY]}{dt} = k_{LH\ XY} X_S \cdot Y_S \frac{A}{V_R} \tag{9}$$

where the rate coefficient $k_{LH\ XY}$ is given by :

$$k_{LH\ XY} = \frac{\upsilon}{4C_{sat}} e^{-E_{LH}/k_B \cdot T_w} \tag{10}$$

with T_w, the wall temperature (typically 300 K), ν, a characteristic frequency [61], which has been assumed to be $\nu \approx 10^{13}$ s^{-1}, and E_{LH}, the global activation energy for this process [62].

Although both the ER and LH mechanisms were incorporated into the kinetic model, the analysis of the results showed that only ER recombination was relevant for the systems considered in this work (see below).

4. Results and discussion

The mass spectra of neutrals in the discharge are dominated by the peaks of the precursor species, but an appreciable amount of HD is also formed in the plasmas of H_2/D_2 mixtures. The relative concentrations of the three neutrals (H_2, D_2 and HD) derived from the measured mass spectra are displayed in Figure 1 for the five mixture proportions varying from 100% D_2 to 100% H_2, and for the two extreme pressures, 1 and 8 Pa (the results for 2 Pa are very similar to those for 1 Pa and are not shown for brevity). The symmetry of the Figure reflects the regular variation in the initial precursor concentrations.

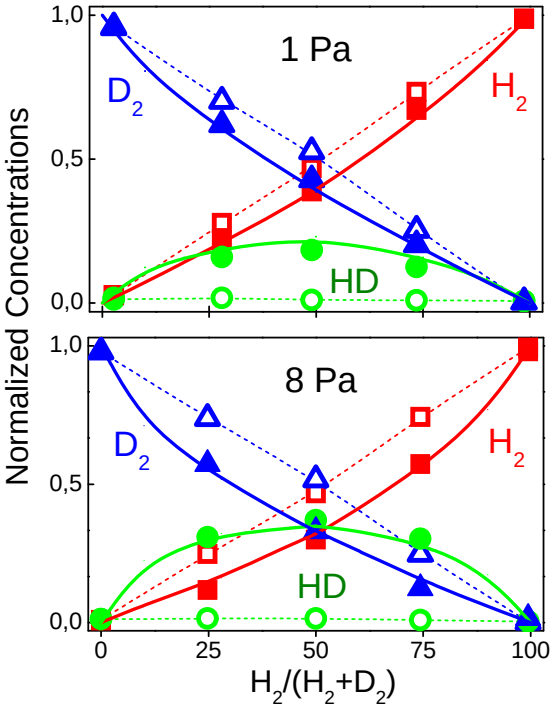

Fig. 1. Relative concentrations of molecules in the reactor before (open symbols) and after (closed symbols) the ignition of the discharge, for 1 and 8 Pa and different $H_2/(H_2+D_2)$ ratios. The symbols represent experimental measurements (squares: H_2, triangles: D_2, circles: HD). Solid lines correspond to the model results for the different plasma compositions. Dashed lines are only to guide the eye in the no-discharge condition.

Under the low pressure conditions of our measurements, characterized by a practical absence of three body collisions in the gas phase, HD is formed through wall recombination of H and D atoms. The relative amount of HD hardly varies when the pressure is increased from 1 to 2 Pa, but grows significantly when the pressure is raised to 8 Pa. In fact, for this pressure, equivalent amounts of H_2, D_2 and HD are obtained in the equimolecular mixture. The analysis of these results with the kinetic model indicates that a significant fraction of the H_2 and D_2 precursor molecules are readily dissociated by electron impact, liberating H and D atoms that flow to the walls, where a high surface coverage of chemisorbed H(s) and D(s) atoms is soon attained. Subsequent flow of atoms from the plasma leads to molecular recombination via an ER mechanism. The concurrence of other mechanisms, and notably LH recombination, to the surface kinetics is not deemed relevant for our system, as discussed below. The experiments do not allow a discrimination between the H_2 and D_2 molecules recycled at the wall and those introduced with the feed gas to the discharges, but the amount of steady state HD produced for the different mixtures and pressures provides a useful gauge of the recombination kinetics. The results of the measurements show that most of the H_2 and D_2 in the fuel gas are dissociated (with characteristic times ~ 0.04 - 0.07 s, which depend on N_e and $\boldsymbol{k_{D_i}(T_e)}$ (see table 2)); and that these precursors are recycled before leaving the reactor chamber (with residence times ~ 0.12 - 0.3 s, depending on the gas pressure). As for the increase of the relative amount of HD with pressure, it is a direct consequence of the higher residence time. The probability of abstraction of an H(s) atom by an impinging hydrogen atom is found to be approximately $\gamma_{ER H_2} = 1.5\times10^{-3}$, somewhat lower than the value reported for the analogous process on films of hydrogenated amorphous carbon (a-C:H) [63,64]. This relatively low abstraction probability, typical for ER reactions, results in a high atomic fraction in the plasma, as shown in Figure 2, where the whole model distribution of neutral species, including the H and D atoms, is represented for the 50% H_2/D_2 mixture at 1 and 8 Pa. In fact, characteristic recombination times, determined from the model, are ~ 0.04 s, which hardly vary with gas pressure and compete with the characteristic dissociation times. Although no atomic concentrations where measured in the present work, the results are consistent with the high fraction of atomic hydrogen estimated from emission spectroscopy measurements for plasmas of pure H_2 [44].

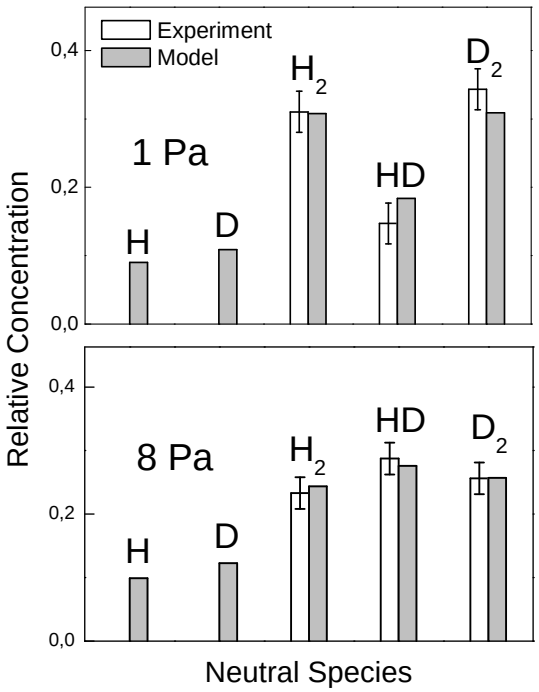

Figure 2. Experimental measurements and model calculations of the relative concentrations of neutral species in the H_2/D_2 (50%) mixture. Upper panel, for a pressure of 1Pa. Lower Panel, for a pressure of 8 Pa. The experimental and theoretical distributions have been put to scale by normalizing the sum of the signals corresponding to the molecular masses 2, 3 and 4, for which measurements are available.

The abstraction efficiency in our experiments was also found to be isotope dependent, as expected for an ER mechanism [14,25,26,64]. The best agreement with the experimental data was obtained by assuming a higher probability (~ 33%) for the abstraction of adsorbed atoms by D ($\gamma_{ER\,D_2} = \gamma_{ER\,DH} = 2\times10^{-3}$) than by H ($\boldsymbol{\gamma_{ER\,H_2} = \gamma_{ER\,HD} = 1.5\times10^{-3}}$), as indicated in the previous section and in table 3, in line with the observations from the literature [14,25]. In order to verify this isotope effect in a more direct way, additional experiments were performed. In these experiments, the chamber walls were first covered with H(s) atoms by exposing them to plasmas of pure H_2. After that, H_2 was removed and the formation of HD in a pure D_2 discharge was observed. The experiment was then repeated for D(s) coverage and a subsequent H_2 discharge. The results, evincing that HD is more efficiently formed in the ER abstraction of H(s) by D atoms, are displayed in Figure 3.

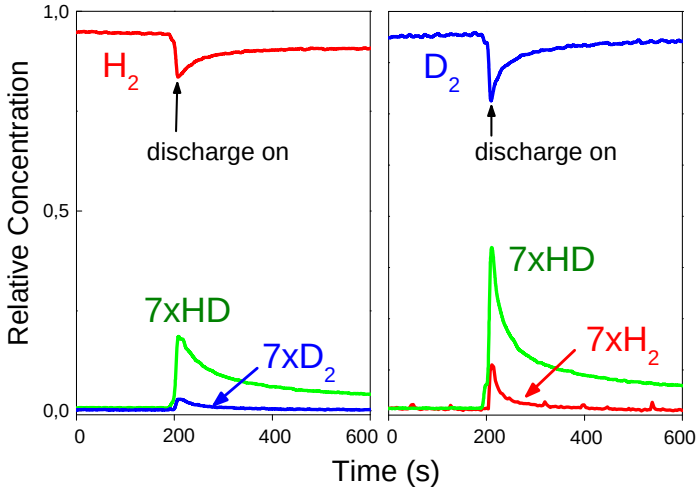

Figure 3. Isotope effect in the HD formation in wall reactions. Left panel: Evolution of molecular concentrations for a H_2 discharge with reactor walls covered by D(s) atoms. Right panel: D_2 discharge with reactor walls covered by H(s) atoms (see text).

The figure also shows that a small amount of H_2 is produced in the D_2 discharge when the walls are covered with H(s) and, conversely, D_2 molecules are also formed in the H_2 discharge with a D(s) covered surface. This result could be due to reactions of gas phase atoms dissociated from the freshly formed HD molecules or to some participation of a hot atom mechanism [22,23] in the heterogeneous discharge chemistry. This mechanism would allow the energy transfer from gas phase atoms to adsorbed atoms which would then react with other atoms of the same kind at the surface, generating the small amount of homonuclear molecules observed. In our case, this reaction pathway is of little relevance for the overall reactivity and has been neglected in the kinetic model. Likewise, dissociative adsorption of $H_2(D_2)$ molecules and subsequent reaction is much less favourable than the direct reaction with gas phase atoms from the plasma and has been also disregarded (see the two panels of figure 3 before the discharge is turned on, where the HD signal is negligible).

A significant contribution of a LH mechanism to molecular recombination in our plasmas is unlikely too. Besides the just mentioned observation of an isotope effect supporting ER abstraction, checks performed with the kinetic model show that pure LH recombination cannot reproduce the observed concentration of gas-phase species. This is illustrated in Figure 4, for the case of the 50% H_2/D_2 mixture at a pressure of 8 Pa, which represents the evolution of the predicted concentrations of neutrals and ions as a function of the activation energy, E_{LH}, assumed for the Langmuir-Hinshelwood recombination. As can bee seen, with a pure LH mechanism the model is unable to

reproduce the measurements, irrespective of the E_{LH} value used. A similar bad agreement between the measurements and the calculations is obtained for the rest of the pressures and mixture proportions studied (not shown for brevity).

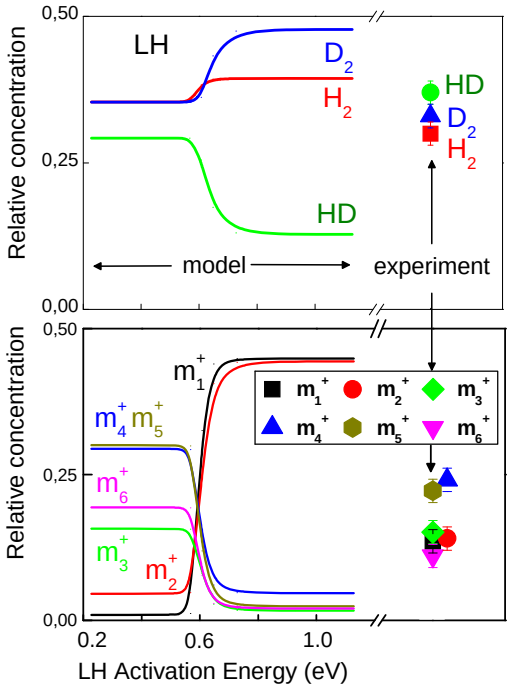

Figure 4 Kinetic model results (lines) for pure Langmuir-Hinshelwood wall recombination as a function of the effective activation energy for this mechanism. The calculations correspond to a pressure of 8 Pa and to a 50% H_2/D_2 mixture. The symbols represent the experimental values. The upper panel displays the results for the neutral molecules and the lower panel those for the ionic species. In each panel the sum of the concentrations has been normalized to one.

When both ER and LH mechanisms are considered together (see Figure 5), the model shows that the LH mechanism would determine surface kinetics only for relatively low values of E_{LH}, and that the ER one would dominate for high E_{LH} activation energies. The switch between the two mechanisms is found to be very abrupt and a significant contribution of both is only found for a narrow E_{LH} range around the switching point, which lies at ~ 0.7 eV. The inability of LH predictions to account for the experimental data suggests that in our system the effective LH activation energy, which may contain contributions from different processes like diffusion and chemical reaction [62], should be higher than this value. Subsurface processes [10,11], are also not included explicitly in the model, which constitutes, no doubt, a simplification of the actual physical problem, but the global good agreement between observations and simulations for the diversity of

cases studied, suggests that, in spite of its approximations, the ER mechanism included in the model captures the essence of the atomic recombination at the walls.

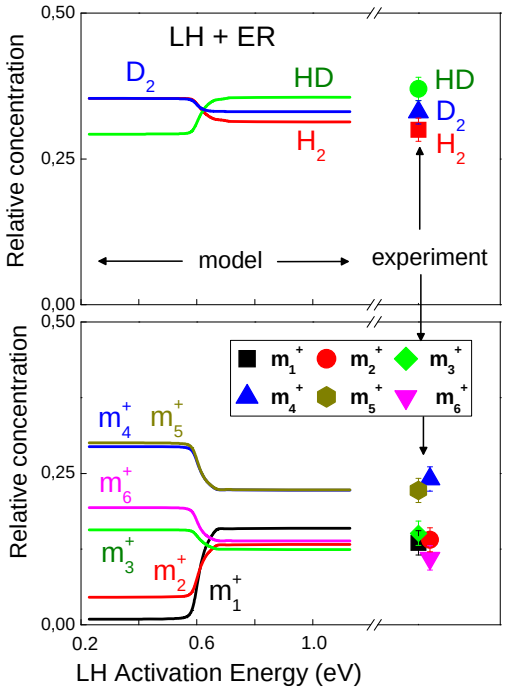

Figure 5 Same as Figure 4, but for a kinetic model including, both Langmuir-Hinshelwood and Eley-Rideal recombination mechanisms. The model results for a LH activation energy higher than 0.7 eV, which are in good agreement with the measurements, are virtually due to the ER mechanism (see text).

The gas phase chemistry in the discharges considered is essentially limited to ion-molecule processes. Reactions between the stable diatomic molecules at room temperature can be confidently excluded, and those between hydrogen atoms and molecules have a very low probability for all the isotopic variants [65,66], even taking into account the vibrational excitation ($T_v \approx 3000$ K) estimated for this type of discharges [44,53,67]. On the other hand, the ions primarily produced by electron impact can be efficiently transformed in encounters with the more abundant neutral species in the plasma, since the large rate coefficients for ion-molecule reactions (see table 2) compensate the low gas-phase collision frequency.

Figure 6 shows the ion-mass distributions measured for the different mixture proportions at 1 and 8 Pa, together with the corresponding model simulations. Masses 1 to 6 are recorded. Three of these masses, m=1, m=5, and m=6, can be directly assigned to the single ions H^+, HD_2^+ and D_3^+ respectively. The other masses correspond to mixed ion signals: m=2 to H_2^+ and D^+, m=3 to H_3^+ and HD^+, and m=4 to D_2^+ and H_2D^+. For discharges of pure H_2 and D_2, the assignment of the different masses is univocal. As can be seen, the kinetic model gives a good global description of

the ion chemistry over the wide range of experimental conditions investigated. A similar degree of agreement between model and measurements is also obtained for the experiments carried out at 2 Pa (not shown for brevity), which produce ionic distributions intermediate between those of 1 Pa and 8 Pa.

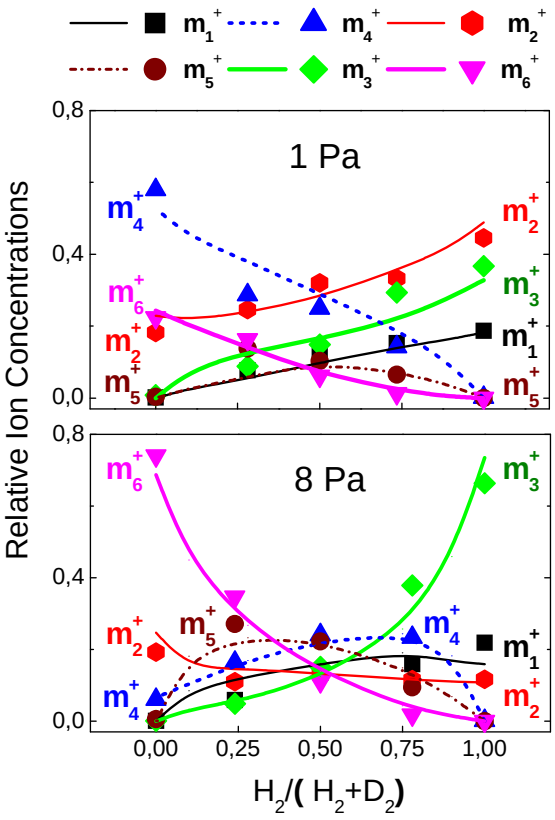

Figure 6. Relative ion concentrations in the plasma for the different mixture proportions at 1 Pa (upper panel) and 8 Pa (lower panel). The symbols represent experimental measurements for the various ion masses. The solid lines correspond to the model calculations.

The pressure increase from 1 to 8 Pa leads to significant changes in the ion distributions, which are best appreciated at the right and left extremes of the graph, corresponding to discharges of pure H_2 and pure D_2, respectively. For the pure gases, the distribution evolves with growing pressure from one in which the major ions are the diatomic species H_2^+ and D_2^+ at 1 Pa, to another where the triatomic ions H_3^+ and D_3^+ are clearly predominant at 8 Pa. As discussed in a previous work [45], the reason for this pronounced composition change lies in the competition between electron impact ionization of the molecules (reactions I_7 and I_8 in table 2) and ion-molecule reactions producing the triatomic ions (reactions M_5 and M_6). The rate of electron impact ionization is strongly dependent on T_e, as reflected by the approximate Arrhenius like rate coefficient included in table 2. At a pressure of 1 Pa, the electron temperature is $T_e \sim 7.6$ eV and the generation of H_2^+ and D_2^+ by electron impact prevails over their destruction in collisions with H_2 and D_2. At this pressure,

corresponding to a molecular density of ~ 2.4 $\times 10^{14}$ cm^{-3}, many of the diatomic ions formed in the plasma leave the glow without gas phase reactions and are neutralized at the wall. At a pressure of 8 Pa, the electron temperature drops to ~ 4 eV and the ensuing decrease, by a factor ~ 10, in the rate of H_2^+ and D_2^+ production cannot compensate the fast transformation of these ions in H_3^+ and D_3^+ through reactions M_5 and M_6. As for the atomic ions in pure H_2 and D_2 discharges, they are produced mainly by direct electron impact ionization from their parent atoms, and, to a lower extent, by the change transfer reactions T_1 and T_2, respectively, which cause also a small decrease in the concentrations of H_2^+ and D_2^+ and a corresponding growth in H^+ and D^+ with increasing pressure. Dissociative ionization processes I_3 and I_4 are of very little relevance.

In the plasmas of gas mixtures, the situation is much more complex, due to the appearance of new ionic species and to the large number of isotopic exchange processes that must be taken into account (see table 2). The set of reactions included in the model and the corresponding rate coefficients are certainly consistent with the experimental data, as shown by the good overall agreement between measurements and calculations for the high number of different cases, with diverse pressures and relative concentrations, considered (figure 6). The contribution of the individual ions to a given mass signal, for those experimentally indistinguishable cases due to their equal masses, can be estimated from the model results, as exemplified in Figure 7 for the H_2/D_2 50% mixture at the lowest and highest pressures studied. Note that, in the case of masses 3 and 4, there is an increase in the proportion of the triatomic ions with respect to their diatomic counterparts when the pressure rises from 1 Pa to 8 Pa, in analogy with the observations discussed above for the plasmas of pure H_2 and D_2. In all cases, mono- and diatomic ions are formed by electron impact ionization of their neutral precursors. This is in fact the only source of diatomic ions considered in our plasma. Monoatomic ions can also be produced through charge exchange (processes T_1-T_6), chemical reactions (M_1-M_4), or very inefficient dissociative ionizations (I_3-I_6). Note that the rate coefficients for reactions M_1-M_4 can vary by an order of magnitude depending on the isotope combination, due to the variation in the zero point energy, ΔZPE, between reactants and products. The two endoergic reactions M_1 and M_2 have appreciably lower rate coefficients than the exoergic processes M_3 and M_4. It should be noted here that these reactions constitute isotopic variants of the $H^+ + H_2$ system, the simplest prototype in studies of ion-molecule reaction dynamics. The reaction takes place through the formation of an H_3^+ complex sustained on a deep (~ 4.5 eV) potential well [68-70], which breaks down eventually to form the products. In spite of the apparent simplicity of the systems involved with just three nuclei and two electrons, many aspects of the dynamics of processes M_1-M_4 are still a challenge for theoretical treatments [71-74], and this is even more so in the case of reactions involving a higher number of atoms.

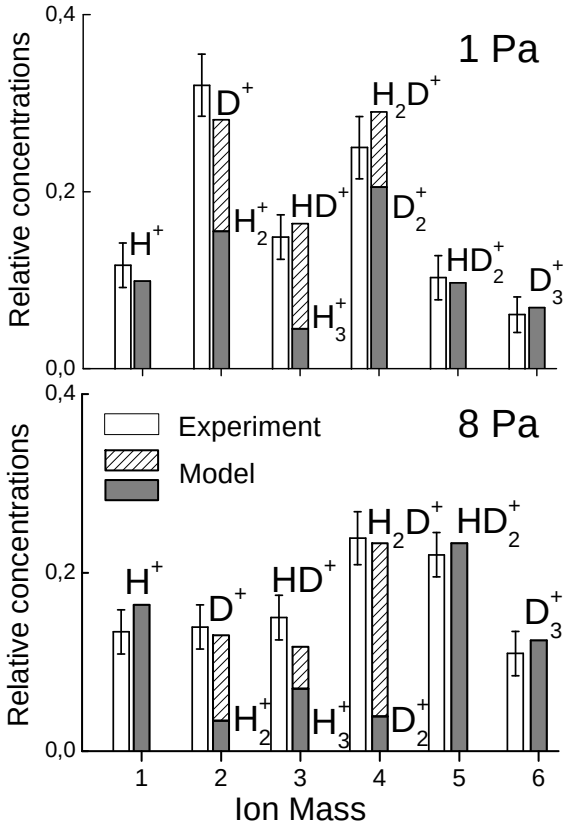

Figure 7 Measured (white bars with error indication) and calculated (grey and striped bars) ion distributions for H_2/D_2 50% mixture plasmas. Upper panel: for a pressure of 1 Pa. Lower panel: for a pressure of 8 Pa. The sum of the signals for each case has been normalized to one. The model calculations allow the separation of the different contributions to the mixed ion signals.

In contrast with their mono and diatomic counterparts, triatomic ions are not produced by electron impact, but are exclusively formed in reactive encounters in the gas phase, and the relevance of these processes increases with growing collision frequency.

Two different pathways can lead to the production of a given triatomic ion, either a direct reaction of a diatomic ion with a neutral molecule (reactions M_5-M_{20}), or isotopic exchange in the collision of a molecule with another triatomic ion (reactions M_{21}-M_{36}). On average, direct reaction of diatomic ions, which are very exothermic (≈ 1.9 eV) and proceed through a direct mechanism [75,76], have somewhat higher rate constants (many of them above 10^{-9} cm^3 s^{-1}) than those of isotope exchange, whose rate coefficients are mostly within the 10^{-10} cm^3 s^{-1} range. It is thus likely that the primary formation processes from the original diatomic precursors have a stronger influence on the final triatomic ion composition, but isotopic redistribution collisions (reactions M_{21}-M_{36}) might also have some effect. Depending on the isotopic variant considered, these reactions are endoergic or exoergic. They proceed via a short lived H_5^+ species (or its deuterated variants), characterized by a shallow potential well [77,78], and the actual reaction probability is

influenced by ZPE constraints, as well as by statistical and dynamical factors pertaining to the formation and breakdown of the H_5^+ intermediate. In fact, ZPE effects in some of these reactions (M_{21}, M_{27} and M_{35}) are assumed to play a decisive role in the chain of increasing deuteration in interstellar space [6,41]. A recent microcanonical model has proven successful for the calculation of rate coefficients at low temperatures [41], but the five-nuclei problem defies at present a rigorous theoretical treatment of the dynamics. Isotope selectivity associated with ZPE effects decreases appreciably with growing T, since the energy required to overcome the ZPE barriers becomes gradually available; but taking into account that typical $\Delta ZPE/k_B$ values for the reactions of interest range between 100 and 250 K [34] (positive or negative, depending on the atomic combination), it is not obvious that all traces of isotopic selectivity should be effaced at room temperature. It is not easy to draw any conclusion in this respect from the direct inspection of table 2, given the relatively high number of reactions implied and the multiplicity of reactive pathways leading to some of the ionic species, but an analysis of specific model results can be helpful.

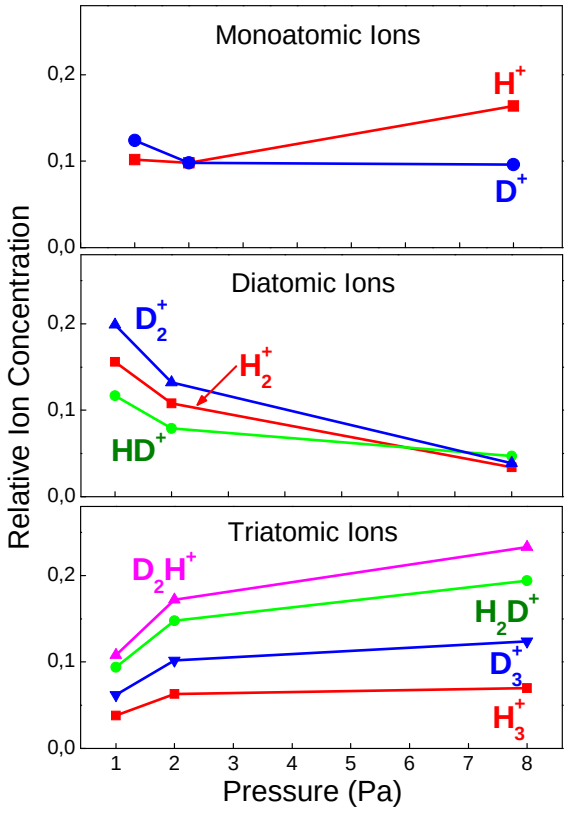

Figure 8 Model distributions of mono- di- and triatomic ions for the H_2/D_2 50% mixture plasmas for pressures of 1Pa, 2Pa and 8 Pa. The sum of all ions at each pressure has been normalized to 1.

Figure 8 displays the ionic distributions calculated with the kinetic model for the H_2/D_2 50% mixtures and for the three pressures studied; mono- di- and triatomic ions are grouped separately for convenience. Note the gradual decrease in the global concentration of diatomic ions and the

concomitant increase in that of triatomic ions with growing pressure. As discussed above, the reason for this behaviour lies in the change of balance between electron impact ionization of the neutral molecules, and ion molecule chemistry of the diatomic ions. At the lowest pressure, with higher electronic temperatures, the former prevails, whereas at the highest pressure, with low T_e values, chemical reactions destroy faster the nascent diatomic ions, which are in turn produced at a lower rate. The observation of the ion distribution for a pressure of 8 Pa is specially interesting since, in this case, the concentration of the three diatomic neutrals is similar (see Figure 2) and a possible isotope selectivity in the ionic species would not be obscured by asymmetries in the concentrations of the primary neutral precursors, and would thus be easier to detect. In the distribution of triatomic ions for this pressure, the larger number of reaction pathways leading to the mixed species H_2D^+ and HD_2^+ results in a higher abundance of these ions with respect to their homonuclear counterparts H_3^+ and D_3^+. At first sight, the formation of ions with a higher degree of deuteration seems to be favoured, since the concentrations of D_3^+ and HD_2^+ are larger than those of H_3^+ and H_2D^+ respectively (see lower panel of figure 8). However, there is a natural enrichment of heavier species in the plasma glow associated with the faster loss of the light ions, which is in principle inversely proportional to the square root of the ionic mass (equation 1). The just mentioned effect is unrelated to the possible D fractionation of chemical origin that we are considering, and must be discounted before any conclusions can be drawn. This is done in Figure 9, which shows the calculated concentrations of triatomic ions divided by the square root of their respective masses. The model calculations (grey bars) predict still a very slight preponderance of the ions with a higher degree of deuteration, due to a residual influence of ZPE constraints at room temperature, but the effect is very small and certainly undetectable in our experimental measurements. It is instructive to consider at this point the separate contribution of the reactions of di- and triatomic ions (reactions M_5-M_{20} and M_{21}-M_{36} respectively) to the shape of the calculated distribution. This is done by removing the reactions of triatomic ions from the model calculations. The predictions of the model without these reactions are also displayed in Figure 9 (white bars).

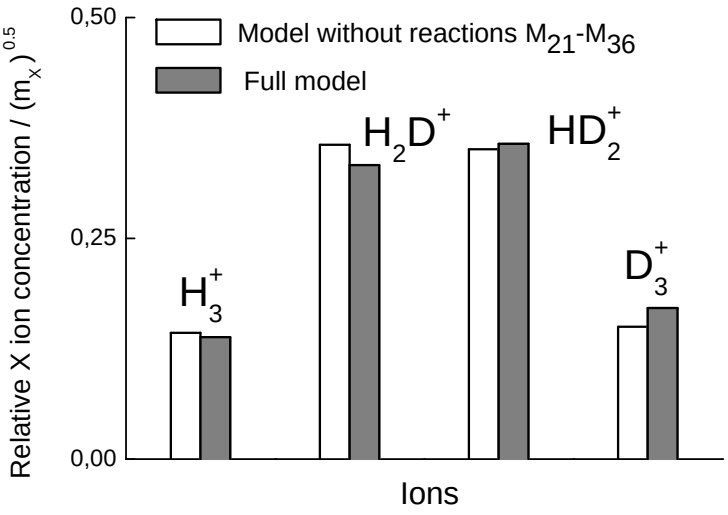

Figure 9 Calculated relative intensities of triatomic ions divided by the square root of their respective masses (see text) for the 50% H_2/D_2 mixture at 8 Pa. Grey bars, full model calculations. White bars, model without reactions of isotopic rearrangement of the triatomic ions (M_{21}-M_{36}). The sum of the corrected intensities has been normalized to one.

The new distribution is very similar to the previous one, but is totally symmetric, without a bias for higher deuteration. This result indicates that the reactions leading primarily to the production of the triatomic ions (M_5-M_{20}) determine essentially the final distribution, whose most salient feature is the much higher proportion of mixed ions. Isotopic rearrangement of the formed ions in subsequent collisions with molecules (M_{21}-M_{36}) has a very small effect and leads only to a barely appreciable enhancement in the relative amount of triatomic ions with a higher D content. The suppression of reactions M_{21}-M_{36} has no effect on the calculated intensities of mono- and diatomic ions.

Isotope selective effects can be identified however at the other end of the ion mass distribution. As shown in the upper panel of Figure 8, the calculated amount of H^+ at 8 Pa is higher than that of D^+, which is in principle unexpected if one takes into account the inverse proportion of their main neutral precursors, H and D (see the lower panel of Figure 2). The predominance of H^+ is enhanced if one discounts the relative enrichment in the heavier D^+ ions due to their lower mobility, as described in the previous paragraph. The corrected values are shown as grey bars in Figure 10.

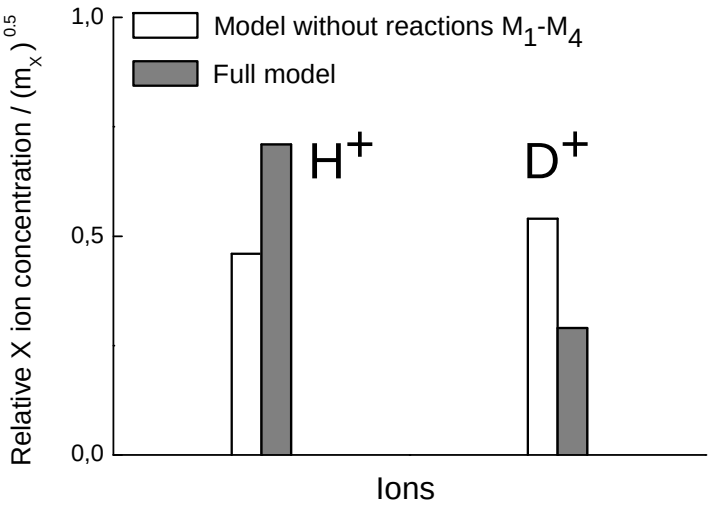

Figure 10 Calculated relative intensities of monoatomic ions divided by the square root of their respective masses (see text) for the 50% H_2/D_2 mixture at 8 Pa. Grey bars, full model calculations. White bars, model without proton (deuteron) exchange reactions (M_1-M_4). The sum of the corrected intensities has been normalized to one.

A detailed analysis shows that the proton (deuteron) exchange reactions M_1 to M_4 are at the root of this effect. The two processes leading to D^+ ions (M_1 and M_2) are endoergic by ≈ 36 and 42 meV (417 and 487 K) respectively, and are neatly slower than the reactions producing H^+ (M_3 and M_4), which are exoergic by the same amount. In this case, ZPE effects add up constructively in the small set of reactions ultimately responsible for the reorganization of H^+ and D^+ ions in the plasma. The suppression of these processes in the model calculations does not affect the results for di- and triatomic ions (not shown), but leads to a large change in the H^+/D^+ ratio, which becomes now very similar to that of the corresponding neutral precursors (see lower panel of Figure 2). The near equality of the experimental signals for ions of masses one and two in the 8 Pa 50% H_2/D_2 plasma (see lower panel of Figure 7) provides evidence for the just described selective H^+ enrichment. In the absence of this effect, the signal of mass two, which corresponds to the slower D^+ ions and contains in addition a contribution of H_2^+, would be significantly larger than that of mass one.

Summary and conclusions

The extensive isotope exchange taking place in low pressure cold plasmas of H_2/D_2 mixtures has been investigated through the diagnostics and modelling of hollow cathode discharges with different pressures and mixture proportions. Quadrupole mass spectrometry was used for the measurement of the distributions of both neutral molecules and ions, and electrical probes were

employed for the estimate of electron temperatures and densities. The varying plasma compositions obtained for the different discharges could be successfully reproduced with a simple zero order kinetic model including gas-phase and heterogeneous chemistry. The good global agreement between measurements and simulations over the wide range of conditions sampled indicates that the model and the associated set of rate coefficients (mostly from bibliographic sources) provide a consistent picture of the kinetics and can be used for the identification of the basic processes determining the observed discharge compositions.

The chemistry of neutral species is dominated by wall recombination of the atoms generated by electron impact dissociation in the discharge glow. This process results in an extensive molecular recycling, leading to newly formed H_2, D_2 and HD. The evolution of the latter molecule (not present in the initial fuel gas) with experimental conditions, provides most valuable information about the relevant surface processes. Under the high atomic flux and large surface coverage characteristic of our experiments, recombination on the stainless steel walls of the reactor is found to proceed essentially through an Eley-Rideal mechanism. The abstraction probability of an adsorbed atom by an impinging gas phase atom is of the order of 10^{-3}. In accordance with previous reports in the literature, an isotopic effect, favouring abstraction by incoming D atoms as compared with H atoms, is also found. The comparison between model predictions and measurements rules out an appreciable contribution of a Langmuir-Hinshelwood mechanism to the surface recombination.

The plasma ions are exclusively produced in the gas-phase, since the (cathode) walls act as an effective sink for the positive charges. The ionic composition in the discharges is largely determined by a competition between electron impact dissociation, prevailing at low pressures, where electron temperatures are higher, and ion-molecule chemistry dominant at the higher pressure. The difference between these two regimes is evinced by the predominance of di- or triatomic ions respectively. The analysis of selected cases at the higher pressure, where chemical reactions are predominant, shows that the distribution of triatomic ions is essentially determined by their primary formation processes in reactions of the diatomic ions (H_2^+, D_2^+ and HD^+) with the diatomic molecules (H_2, D_2 and HD). In these reactions, the formation of mixed ions of the type X_2Y^+ is favoured over that of their homonuclear counterparts, as expected on statistical grounds, but no isotopic preference is observed. The model results suggest that subsequent isotopic rearrangement of the triatomic ions in further ion-molecule collisions can lead to a tiny relative enrichment in the molecules with higher deuteration. This effect, which is very small and within the uncertainty of our room temperature experiments, is a likely residual influence of the ZPE constraints, assumed to play a key role for this type of reactions at the very low temperature of interstellar environments. Isotope selective ZPE effects are however clearly manifest, even for the present room temperature experiments, in the ratio of monoatomic ions in the plasma. The exoergic

reactions of D^+ with H_2 and HD, which produce H^+, are favoured in comparison with the analogous endoergic processes $H^+ + D_2$ and $H^+ + HD$, which lead to the formation of D^+.

Acknowledgements

This work has been funded by the MICINN of Spain under projects FIS 2007-61686, FIS2010-16455 and CSD2009-00038. EC acknowledges also funding from the JdC program of the MICINN. M. A. Moreno, J. Rodríguez and D. Pérez are acknowledged for technical support.

Table 1. Electron temperatures and concentrations, both, obtained experimentally by the Langmuir probe, and giving the best fittings to neutral and ion concentrations in the model.

Pressure (Pa)	Te (eV, experiment)	Te (eV, model)	Ne (cm^{-3}, experiment and model)
1	7.0±1	7.6	$(0.8\pm0.15)\times10^{10}$
2	5.5±1	5.8	$(1.0\pm0.2)\times10^{10}$
8	4.0±0.8	4.2	$(1.5\pm0.3)\times10^{10}$

Table 2. Homogeneous reactions

Nº	Process	Rate constant ($cm^3\ s^{-1}$)	Source
	Electron Impact Dissociation		
D_1	$H_2 + e^- \rightarrow 2H + e^-$	$1.75\times10^{-7} \times T_e^{-1.23} \times e^{-12.59/Te}$	a
D_2	$D_2 + e^- \rightarrow 2D + e^-$	$1.75\times10^{-7} \times T_e^{-1.23} \times e^{-12.59/Te}$	b
D_3	$HD + e^- \rightarrow H + D + e^-$	$1.75\times10^{-7} \times T_e^{-1.23} \times e^{-12.59/Te}$	b
	Electron Impact Ionization		
I_1	$H + e^- \rightarrow H^+ + 2e^-$	$6.50\times10^{-9} \times T_e^{0.49} \times e^{-12.89/Te}$	a
I_2	$D + e^- \rightarrow D^+ + 2e^-$	$6.50\times10^{-9} \times T_e^{0.49} \times e^{-12.89/Te}$	c
I_3	$H_2 + e^- \rightarrow H^+ + H + 2e^-$	$3.00\times10^{-8} \times T_e^{0.44} \times e^{-37.73/Te}$	a
I_4	$D_2 + e^- \rightarrow D^+ + D + 2e^-$	$3.00\times10^{-8} \times T_e^{0.44} \times e^{-37.73/Te}$	d
I_5	$HD + e^- \rightarrow H^+ + D + 2e^-$	$0.5\times3.00\times10^{-8} \times T_e^{0.44} \times e^{-37.73/Te}$	e
I_6	$HD + e^- \rightarrow D^+ + H + 2e^-$	$0.5\times3.00\times10^{-8} \times T_e^{0.44} \times e^{-37.73/Te}$	e
I_7	$H_2 + e^- \rightarrow H_2^+ + 2e^-$	$3.12\times10^{-8} \times T_e^{0.17} \times e^{-20.08/Te}$	a
I_8	$D_2 + e^- \rightarrow D_2^+ + 2e^-$	$3.12\times10^{-8} \times T_e^{0.17} \times e^{-20.08/Te}$	f
I_9	$HD + e^- \rightarrow HD^+ + 2e^-$	$3.12\times10^{-8} \times T_e^{0.17} \times e^{-20.08/Te}$	f
	Charge Transfer		
T_1	$H_2^+ + H \rightarrow H_2 + H^+$	6.40×10^{-10}	a
T_2	$D_2^+ + D \rightarrow D_2 + D^+$	5.00×10^{-10}	g
T_3	$HD^+ + H \rightarrow HD + H^+$	5.00×10^{-10}	h
T_4	$HD^+ + D \rightarrow HD + D^+$	5.00×10^{-10}	h
T_5	$H_2^+ + D \rightarrow H_2 + D^+$	6.40×10^{-10}	i
T_6	$D_2^+ + H \rightarrow D_2 + H^+$	5.00×10^{-10}	h
	Ion-Molecule Reaction		
M_1	$H^+ + HD \rightarrow D^+ + H_2$	1.70×10^{-10}	g
M_2	$H^+ + D_2 \rightarrow D^+ + HD$	3.60×10^{-10}	g
M_3	$D^+ + H_2 \rightarrow H^+ + HD$	1.40×10^{-9}	g
M_4	$D^+ + HD \rightarrow H^+ + D_2$	9.50×10^{-10}	g
M_5	$H_2^+ + H_2 \rightarrow H_3^+ + H$	2.00×10^{-9}	g
M_6	$D_2^+ + D_2 \rightarrow D_3^+ + D$	1.60×10^{-9}	g
M_7	$H_2^+ + D_2 \rightarrow H_2D^+ + D$	$0.50\times3.20\times10^{-9}$	j
M_8	$H_2^+ + D_2 \rightarrow HD_2^+ + H$	$0.50\times3.20\times10^{-9}$	j
M_9	$D_2^+ + H_2 \rightarrow H_2D^+ + D$	$0.50\times3.00\times10^{-9}$	j
M_{10}	$D_2^+ + H_2 \rightarrow HD_2^+ + H$	$0.50\times3.00\times10^{-9}$	j
M_{11}	$H_2^+ + HD \rightarrow H_2D^+ + H$	$0.75\times2.00\times10^{-9}$	k
M_{12}	$H_2^+ + HD \rightarrow H_3^+ + H$	$0.25\times2.00\times10^{-9}$	k
M_{13}	$D_2^+ + HD \rightarrow HD_2^+ + D$	$0.67\times1.80\times10^{-9}$	l
M_{14}	$D_2^+ + HD \rightarrow D_3^+ + H$	$0.33\times1.80\times10^{-9}$	l
M_{15}	$HD^+ + HD \rightarrow H_2D^+ + D$	0.80×10^{-9}	m
M_{16}	$HD^+ + HD \rightarrow HD_2^+ + H$	1.00×10^{-9}	m
M_{17}	$HD^+ + H_2 \rightarrow H_2D^+ + H$	$0.75\times2.00\times10^{-9}$	k
M_{18}	$HD^+ + H_2 \rightarrow H_3^+ + D$	$0.25\times2.00\times10^{-9}$	k
M_{19}	$HD^+ + D_2 \rightarrow HD_2^+ + D$	$0.66\times2.00\times10^{-9}$	l
M_{20}	$HD^+ + D_2 \rightarrow D_3^+ + H$	$0.33\times2.00\times10^{-9}$	l
M_{21}	$H_3^+ + HD \rightarrow H_2D^+ + H_2$	9.60×10^{-10}	n
M_{22}	$H_2D^+ + H_2 \rightarrow H_3^+ + HD$	5.30×10^{-10}	n
M_{23}	$H_3^+ + D_2 \rightarrow H_2D^+ + HD$	2.60×10^{-10}	n
M_{24}	$H_2D^+ + HD \rightarrow H_3^+ + D_2$	5.00×10^{-11}	n
M_{25}	$H_3^+ + D_2 \rightarrow HD_2^+ + H_2$	1.00×10^{-9}	n

M_{26}	$HD_2^+ + H_2 \rightarrow H_3^+ + D_2$	1.90×10^{-10}	n
M_{27}	$H_2D^+ + HD \rightarrow HD_2^+ + H_2$	4.50×10^{-10}	n
M_{28}	$HD_2^+ + H_2 \rightarrow H_2D^+ + HD$	5.70×10^{-10}	n
M_{29}	$H_2D^+ + D_2 \rightarrow HD_2^+ + HD$	6.50×10^{-10}	n
M_{30}	$HD_2^+ + HD \rightarrow H_2D^+ + D_2$	3.40×10^{-10}	n
M_{31}	$H_2D^+ + D_2 \rightarrow D_3^+ + H_2$	3.50×10^{-10}	n
M_{32}	$D_3^+ + H_2 \rightarrow H_2D^+ + D_2$	5.30×10^{-10}	n
M_{33}	$HD_2^+ + HD \rightarrow D_3^+ + H_2$	1.10×10^{-10}	n
M_{34}	$D_3^+ + H_2 \rightarrow HD_2^+ + HD$	2.90×10^{-10}	n
M_{35}	$HD_2^+ + D_2 \rightarrow D_3^+ + HD$	5.20×10^{-10}	n
M_{36}	$D_3^+ + HD \rightarrow HD_2^+ + D_2$	6.60×10^{-10}	n

T_e is given in eV. a) References [44,50]; b) same as D_1; c) same as I_1; d) same as I_3; e) same as I_3, considering the statistical branching ratio; f) same as I_7; g) reference [43]; h) same as T_2; i) same as T_1; j) reference [43], considering the statistical branching ratio; k) estimated from reference [79], considering the statistical branching ratio; l) branching ratio from [80], rate coefficient estimated from cross section in the same reference; m) from reference [81]; n) from reference [34].

Table 3 Wall neutralization and heterogeneous reactions

	Wall Neutralization		
W_1	$H^+ + wall \rightarrow H$	Eqn. 1	See text
W_2	$H_2^+ + wall \rightarrow H_2$	Eqn. 1	"
W_3	$H_3^+ + wall \rightarrow H_2 + H$	Eqn. 1	"
W_4	$D^+ + wall \rightarrow D$	Eqn. 1	"
W_5	$D_2^+ + wall \rightarrow D_2$	Eqn. 1	"
W_6	$D_3^+ + wall \rightarrow D_2 + D$	Eqn. 1	"
W_7	$H_2D^+ + wall \rightarrow H_2 + D$	Eqn. 1	"
W_8	$HD_2^+ + wall \rightarrow D_2 + H$	Eqn. 1	"
W_9	$H_2D^+ + wall \rightarrow HD + H$	Eqn. 1	"
W_{10}	$HD_2^+ + wall \rightarrow HD + D$	Eqn. 1	"
W_{11}	$HD^+ + wall \rightarrow HD$	Eqn. 1	"
	Heterogeneous Reactions		
H_1	$H + wall \rightarrow H(s)$	Eqs. 2-5; $\gamma_{ads}=1$	See text
H_2	$D + wall \rightarrow D(s)$	Eqs. 2-5; $\gamma_{ads}=1$	"
H_3	$H + H(s) \rightarrow H_2$	Eqs. 7-8; $\gamma_{ER\ H2}=1.5\times10^{-3}$	"
H_4	$D + H(s) \rightarrow HD$	Eqs. 7-8; $\gamma_{ER\ DH}=2.0\times10^{-3}$	"
H_5	$H + D(s) \rightarrow HD$	Eqs. 7-8; $\gamma_{ER\ HD}=1.5\times10^{-3}$	"
H_6	$D + D(s) \rightarrow D_2$	Eqs. 7-8; $\gamma_{ER\ H2}=2.0\times10^{-3}$	"

References

[1] G. Federici, C. H. Skinner, J. N. Brooks, J. P. Coad ,C. Grisolia, A. A. Haasz, A. Hassanein, V Philipps, C. S. Pitcher, J. Roth, W. R. Wampler and D. G. Whyte, *Nucl. Fusion* 2001, **41**, 1967.

[2] U. Samm, *Contemp. Phys.* 2003, **44**, 203.

[3] D. L. Huestis, S. W. Bougher, J. L. Fox, M. Galand, R. E. Johnson, J. I. Moses, and J. C. Pickering, *Space Sci. Rev*. 2008, **139**, 63.

[4] S. N. Tripathi, M. Michael and R. G. Harrison, *Space Sci. Rev*. 2008, **137**, 193.

[5] E. Herbst, *Chem. Soc. Rev.* 2001, **30**, 168.

[6] T. J. Millar, *Astron. Geophys.* 2005, **46**, 2.29.

[7] F. J. Gordillo-Vázquez, V. J. Herrero, I. Tanarro, *Chem. Vap. Deposition*, 2007, **13**, 267.

[8] L. Hornekaer, A. Baurichter, V. V. Petrunin, D. Field and A. C. Luntz, *Science*, 2003, **302**, 1943.

[9] E. Herbst, *J. Phys. Chem. A*, 2005, **109**, 4017.

[10] M. A. Pick and K. Sonnenberg, *J. Nucl. Mater.* 1985, **131**, 208.

[11] A. Winkler, *Appl. Phys. A*, 1998, **67**, 637.

[12] N. Katz, I. Furman, O. Biham, V. Pirronello, G. Vidali, *Astrophys. J* 1999, **522**, 305.

[13] S. Cazaux and A. G. G. M. Tielens, *Astrophys. J*, 2004, **604**, 222.

[14] M. Rutigliano and M. Cacciatore, *Chem.* Phys. *Chem*. 2008, **9**, 171.

[15] M Cacciatore and M. Rutigliano, *Plasma Sources Sci Technol.* 2009, **18**, 023002.

[16] J. I. Steinfeld, J. S. Francisco and W. L. Hase, *Chemical Kinetics and Dynamics*, 1999 (Prentice and Hall).

[17] K. W. Kolasinski, *Surface Science*, 2002 (John Wiley & Sons).

[18] B. Kerkeni, D. C. Clary, *Chem. Phys.* 2007, **338**, 1.

[19] C. T. Rettner, *Phys. Rev. Lett.* 1992, **69**, 383.

[20] C. T. Rettner and D. J. Auerbach, *Science* 1994, **263**, 365.

[21] C. T. Rettner J. Chem. Phys. 1994, **101**, 1529.

[22] J. Harris and B. Kasemo, *Surf. Sci. Lett.* 1981, **105**, L281.

[23] Th. Kammler, D. Kolovos-Vellianitis and J. Küppers, *Surf. Sci.* 2000, **460**, 91.

[24] V. Guerra, *IEE trans. Plasma Sci.* 2007, **35**, 1397.

[25] M. Persson and B. Jackson, *Chem. Phys. Lett*. 1995, **237**, 468.

[26] B. Jackson and M. Persson, *J. Chem. Phys.* 1992, **96**, 2378.

[27] W. D. Watson, *Rev. Mod. Phys.* 1976, **48**, 513.

[28] D. Gerlich, E. Herbst, E. Roueff, *Planet. Space. Sci.* 2002, **50**, 1275.

[29] D. Gerlich, S. Schlemmer, *Planet. Space. Sci.* 2002, **50**, 1287.

[30] H. Roberts, E. Herbst, and T. J. Millar, *Astrophys. J.* 2003, **591**, L41.

[31] H. Roberts, E. Herbst, and T. J. Millar, *Astron. Astrophys.* 2004, **424**, 905.

[32] R. Stark, F. F. S Van der Tak, E. F. Van Dishoeck, *Astrophys. J.* 1999, **521**, L67.

[33] C. Vastel, T. G. Philips, H. Yoshida, *Astrophys. J.* 2004, **606**, L127.

[34] K. Giles, N. G. Adams, D. Smith, *J. Phys. Chem.* 1992, **96,** 7645.

[35] M. Cordonnier, D. Uy, R. M. Dickson, K. E. Kerr, Y. Zhang, and T. Oka, *J. Chem. Phys.* 2000, **113**, 3181.

[36] T. Oka, *J. Molec. Spectrosc.* 2004, **228**, 635.

[37] J. Ramanlal and J. Tennyson, 2004, *Mon. Not. R. Astronom. Soc.* 2004, **354**, 161.

[38] D. Gerlich, F. Windisch, P. Hlavenka, R. Plašil, J. Glosik, *Phil. Trans. R. Soc.A*, 2006, **364**, 3007.

[39] K. Park and J. C. Light, *J. Chem. Phys.* 2007, **126**, 044305.

[40] K. Park and J. C. Light, *J. Chem. Phys.* 2007, **127**, 224101.

[41] E. Hugo, O. Asvany, S. Schlemmer, *J. Chem. Phys.* 2009, **130**, 164302.

[42] N. G. Adams and D. Smith, *Astrophys. J.* 1981, 248, 373.

[43] V. G. Anicich, *J. Phys. Chem. Ref. Data,* 1993, **22**, 1469. JPL publication 03-19 NASA 2003.

[44] I. Méndez, F. J. Gordillo-Vázquez, V. J. Herrero and I. Tanarro, *J. Phys. Chem. A* 2006, **110**, 6060.

[45] I. Tanarro and V. J. Herrero, *Plasma Sources Sci.Tec.* 2011, in press.
[46] I. Tanarro V. J. Herrero, A. M. Islyaikin, I. Méndez, F. L. Tabarés, D. Tafalla, *J. Phys. Chem. A,* 2007, **111,** 9003.
[47] J. A. Ferreira, Ph D Thesis, Universidad Complutense de Madrid, 2008.
[48] V. J. Herrero, A. M. Islyiakin,d I. Tanarro, *J. Mass Spectrom*. 2008, **43**, 1148. (10.1002/jms.1388)
[49] I. Tanarro, V. J. Herrero, *Plasma Sources Sci.Tec.* 2009, **18**, 034007.
[50] J. Loureiro and C. M Ferreira, *J. Phys. D. Appl. Phys.* 1989, **22**, 1680.
[51] A. Garscadden and R. Nagpal, *Plasma Sources Sci. Technol.* 1995, **4**, 268.
[52] F. J. Gordillo-Vázquez, *J. Phys. D. Appl. Phys.* 2008, **41**, 234016.
[53] E. M. Hollmann, A. Yu Pigarov, *Phys. Plasmas* 2002, **9**, 4330.
[54] M. Capitelli and C. Gorse, *IEEETtrans. Plasma Sci.* 2005, 33, 1832.
[55] V. Gencheva, R. Djulgerova, V. Mihailov, T. Dohnalik, and Z. Lju. Petrovic, *J. Phys. Conf. Ser.* 2007, 71, 012009.
[56] M. Larsson, B. J. McCall, and E. Orel, 2008, *Chem. Phys. Lett.* **462**, 145.
[57] M. Castillo, I. Méndez, A. M. Islyaikin, V. J. Herrero, and I. Tanarro. *J. Phys Chem. A*, 2005, **109**, 6255.
[58] M. A. Liebermann and A. J. Lichtenberg *Principles of Plasma Discharges and Materials Processing*, Wiley & sons, 1994.
[59] P. J. Chantry, *J. Appl. Phys,* 1987, **62**, 1141.
[60] P. Kae-Nune, J. Perrin, J. Jolly and J. Guillo, *Surf. Sci. Lett,* 1996, **360**, L495.
[61] J. V. Barth, *Surf. Sci. Rep,* 2000, **40**, 75.
[62] B. Gordiets, C. M. Ferreira, M. J. Pinheiro and A. Ricard, *Plasma Sources Sci. Technol.* 1998, **7**, 379.
[63] J. Küppers, *Surf. Sci Rep.* 1995, **22**, 249.
[64] A. Von Keudell, *Plasma Sources Sci. Tech.* 2000, **9**, 455.
[65] F. J. Aoiz, V. J. Herrero and V. Sáez Rábanos, *J. Chem. Phys.* 1991, **94**, 7991.
[66] F. J. Aoiz, L. Bañares and V. J. Herrero, *Int. Rev. Phys. Chem,* 2005, **24**, 119.
[67] T. Shikama, S. Kado, Y. Kuwahara, K. Kurihara, F. Scotti, and S. Tanaka, *J. Plasma Fusion Res.* 2007, **2**, S1045.
[68] W. Cenceck, J. Rychlewski, R. Jaquet, and W. Kutzelnigg, *J. Chem. Phys,* 1998, **108**, 2831.
[69] A. Aguado, O. Roncero, C. Tablero, C. Sanz, and M. Paniagua, *J. Chem. Phys.* 2001, **112**, 1240.
[70] H. Kamisaka, W. Bian, K. Nobusada, and H. Nakamura, *J. Chem. Phys.* 2002, **116**, 654.
[71] T. González-Lezana, A. Aguado, M. Paniagua, and O. Roncero, *J. Chem. Phys,* 2005, **123**, 194309.
[72] E. Carmona-Novillo, T. González-Lezana, O. Roncero, P. Honvault, J. M. Launay, N. Bulut, F. J. Aoiz, L. Bañares, A. Trottier, and E. Wrede, *J. Chem.Phys.* 2008, **128**, 014304.
[73] P. G. Jambrina, F. J. Aoiz, N. Bulut, S. C. Smith, G. G. Balint-Kurti, and M. Hankel, *Phys. Chem. Chem. Phys,* 2010, **12**, 1102.
[74] P. G. Jambrina, J. M. Alvariño, F. J. Aoiz, V. J. Herrero, and V. Sáez Rábanos, *Phys. Chem. Chem. Phys,* 2010, **12**, 12591.
[75] S. L. Anderson, F. A. Houle, D. Gerlich, and Y. T. Lee, *J. Chem. Phy,* 1981, **75**, 2153.
[76] C. W. Eaker and G. C. Schatz, *J. Phys. Chem.* 1985, **89**, 2612.
[77] A. Aguado, P. Barragan, R. Prosmiti, G. Delgado-Barrio, P. Villarreal and O. Roncero, *J. Chem. Phys.* **133**, 024306.
[78] P. Barragan, R. Prosmiti, O. Roncero, A. Aguado, P. Villarreal, and G. Delgado-Barrio, *J. Chem. Phys,* 2010, **133**, 054303.
[79] C. A. Picconatto and G. I. Gellene, *J. Phys. Chem.* 1993, **97**, 13629.
[80] C. H. Douglass, D. J. McClure and R. Gentry, *J. Chem. Phys.* 1977, **67**, 4931.
[81] R. P. Clou and J. H. Futrell, *Int. J. Mass Spectrom. Ion Phys.* 1972, **8**, 119.